Ring-Opening-Induced Toughening of a Low-Permittivity Polymer–Metal Interface

B. Singh,[†] S. Garg,[†] J. Rathore,[‡] R. Moore,[§] N. Ravishankar,[†,||] L. Interrante,[‡] and Ganpati Ramanath*[,†]

Materials Science and Engineering Department and Department of Chemistry, Rensselaer Polytechnic Institute, Troy, New York 12180, College of Nanoscale Science & Engineering, State University of New York, Albany, New York 12203, and Materials Research Centre, Indian Institute of Science, Bangalore, India

ABSTRACT Integrating low dielectric permittivity (low-*k*) polymers to metals is an exacting fundamental challenge because poor bonding between low-polarizability moieties and metals precludes good interfacial adhesion. Conventional adhesion-enhancing methods such as using intermediary layers are unsuitable for engineering polymer/metal interfaces for many applications because of the collateral increase in dielectric permittivity. Here, we demonstrate a completely new approach without surface treatments or intermediary layers to obtain an excellent interfacial fracture toughness of >13 J/m^2 in a model system comprising copper and a cross-linked polycarbosilane with $k \sim 2.7$ obtained by curing a cyclolinear polycarbosilane in air. Our results suggest that interfacial oxygen catalyzed molecular ring-opening and anchoring of the opened ring moieties of the polymer to copper is the main toughening mechanism. This novel approach of realizing adherent low-*k* polymer/metal structures without intermediary layers by activating metal-anchoring polymer moieties at the interface could be adapted for applications such as device wiring and packaging, and laminates and composites.

KEYWORDS: low *k* • polymer • interface toughening • ring-opening • carbosilane • copper

1. INTRODUCTION

Designing low-dielectric-permittivity (low-*k*) materials and integrating them with copper are crucial for nanoelectronics device wiring (1, 2), laminates for high-frequency electronics (3), communications and packaging (4), and coatings and composites (5). However, incorporating porosity or low-polarizability moieties to decrease *k* degrades mechanical properties of the dielectric film (6, 7) or renders it less adherent to metals because of weak chemical bonding of low-polarizability moieties with metals. Present solutions based on using intermediary layers to promote adhesion and block metal diffusion (8–10) may not be amenable for emerging technologies. For example, in nanoelectronics devices for integrated circuits, additional layers compromise the advantages of low resistivity copper wiring, or increase device processing and integration complexity. Recent works have shown that dielectric materials derived from polycarbosilanes not only promise ultralow dielectric constants (e.g., as low as 1.8 for porous polycarbosiloxane films) and high mechanical strength (11), but also exhibit excellent thermal stability, e.g., up to at least 300 °C in air (12), and block copper diffusion without an intermediary layer (13).

Here, we demonstrate that a polymeric dielectric with $k \approx 2.7$ obtained by cross-linking of cyclolinear polycarbosilane (CLPCS) can exhibit interfacial toughness >13 J/m^2 with copper, without the use of intermediary layers. Enhanced low-*k* polymer–metal interfacial adhesion in this model system occurs by oxygen-mediated opening of disilacyclobutane (DSCB) rings in the polymer, and covalent anchoring of the opened moieties to the metal during air curing. Vacuum curing scavenges the surface oxygen via copper oxide reduction and precludes the oxygen from anchoring the polymer chains to the metal surface. Although the primary purpose is to demonstrate the validity of our concept for a model metal–polymer interface comprising Cu and CLPCS, we note that the measured fracture toughness for air-curing exceeds the benchmark for integrated circuits (14) and is unprecedented for metal/low-*k* polymer interfaces without interlayers. Our results point to a new way of designing low *k* materials that could be directly integrated with a metal for applications in nanodevice wiring, communications, packaging, coatings, and composites.

2. EXPERIMENTAL DETAILS

We used 600-μm-thick Si(001) wafers capped with a 80-nm-thick thermal silica layer as substrates for creating thin film structures with copper–polycarbosilane interfaces. The substrates were cleaned successively in xylene, acetone, isopropanol and deionized water and dried gently with a nitrogen jet. We created Cu/Ta/Si(001) thin film structures by successively depositing 50-nm-thick Ta and 50-nm-thick Cu layers without a vacuum break in a CVC sputtering tool with a 1×10^{-6} Torr base pressure. The Ta layer was introduced to counteract poor Cu/silica adhesion. We then deposited 300 ± 10-nm-thick CLPCS films by spin-coating a 8 wt % solution of poly[hexam-

* Corresponding author. E-mail: Ramanath@rpi.edu.
Received for review February 24, 2010 and accepted April 14, 2010
[†] Materials Science and Engineering Department, Rensselaer Polytechnic Institute.
[‡] Department of Chemistry, Rensselaer Polytechnic Institute.
[§] State University of New York.
[||] Indian Institute of Science.
DOI: 10.1021/am1001597

ethylene-1,3-(1,3-dimethyl-1,3-disilacyclobutane)] (15) in xylene at 3000 rpm for 100 s onto the Cu film surface. All the CLPCS films were cured at $T_{curing} = 250$ °C for 45 min in air or in a 5×10^{-7} Torr vacuum prior to any further treatment. This temperature−time combination was sufficient for CLPCS cross-linking via disilacyclobutane (DSCB) ring-opening (15), as described later below. Herein, we refer to cured CLPCS as PCS.

Following CLPCS curing, a second 50-nm-thick Ta layer was deposited on PCS. The resultant Ta/PCS/Cu/Ta/Si(001) structures were glued to a dummy silicon wafer using an epoxy to obtain dummy-Si/epoxy/Ta/PCS/Cu/Ta/Si(001) structures. The second Ta layer was used to circumvent poor adhesion between PCS and the epoxy. The thin film stacks were diced into 5 mm ×40 mm beams and notched on the Si(001) substrate for four-point bend tests carried out as described in detail elsewhere (9, 16). During four-point bending, a crack originating at the notch kinks to the weakest interface, at which point we obtain a plateau in the load vs displacement curve (supplementary Figure S1). From the critical load at the plateau, we extract the fracture toughness of the interface using linear elastic fracture mechanics (17, 18). Each interfacial toughness value reported here is an average of at least six measurements.

We note that the use of the Ta glue layers to pre-empt delamination at Cu/silica or epoxy/PCS interfaces is important because premature failure at these interfaces would preclude a direct measure of the PCS−Cu interface toughness. If delamination occurs at some other interface, the measured toughness value would serve as a lower bound estimate for the undelaminated PCS−Cu interface. For the estimate to be useful, however, the measured toughness needs to be as high as possible. Accordingly, we attempted to toughen the delaminating interface by subjecting our test sandwiches to a postcure anneal at different temperatures 150 °C ≤ T_{anneal} ≤ 300 °C prior to four point bend testing. These experiments also provide a means to understand whether or not annealing has an effect on PCS−Cu interfacial toughness in cases where delamination occurs at this interface.

Fracture surface chemistry was studied by X-ray photoelectron spectroscopy (XPS) using a PHI 5400 instrument with a Mg Kα beam. Samples were transferred to the XPS chamber within 5 min of interfacial fracture to minimize spurious surface oxidation and moisture attack. One consequence of this rapid analysis is that our results represent scenarios that are far from equilibrium. The peaks were calibrated using Cu and Au standards, and corrected for charging using the 285 eV adventitious C 1s peak as a marker. We also used XPS to study the chemical changes at the PCS-Cu interface by monitoring the Cu 2p core level and Auger LMM bands during the curing of a very thin ~3−5 nm thick CLPCS layer on a Cu surface. Such low polymer layer thickness is essential to retain the spectral signatures of Cu that would otherwise be lost to the background due to multiple inelastic collisions of the ejected photo- and Auger electrons. The Cu LMM bands were used to distinguish Cu(I) and Cu(0) because the two states exhibit nearly identical Cu 2p bands (19). The Cu(II)/[Cu(I)+Cu(0)] ratio was calculated from intensities of the Cu $2p_{3/2}$ sub-band at 932.4 eV attributable to Cu(0) or Cu(I) and the shoulder sub-band at ~934.5 eV from Cu(II). The Cu(0)/Cu(I) ratio was determined by deconvoluting the respective components from the Cu LMM peak.

Infrared spectra were acquired using a Nicolet Magna IR 560 spectrometer to study cross-linking in the polymer film. The spectra indicate changes in the bulk of the film, but do not capture signatures of chemical changes occurring exclusively at the PCS-Cu interface. The relative dielectric permittivity k was determined by measuring the capacitance of Cu/PCS/n^+-Si metal−insulator−metal structures with different gate diameters between 0.5−1.5 mm using a HP 4140B instrument at 1 MHz.

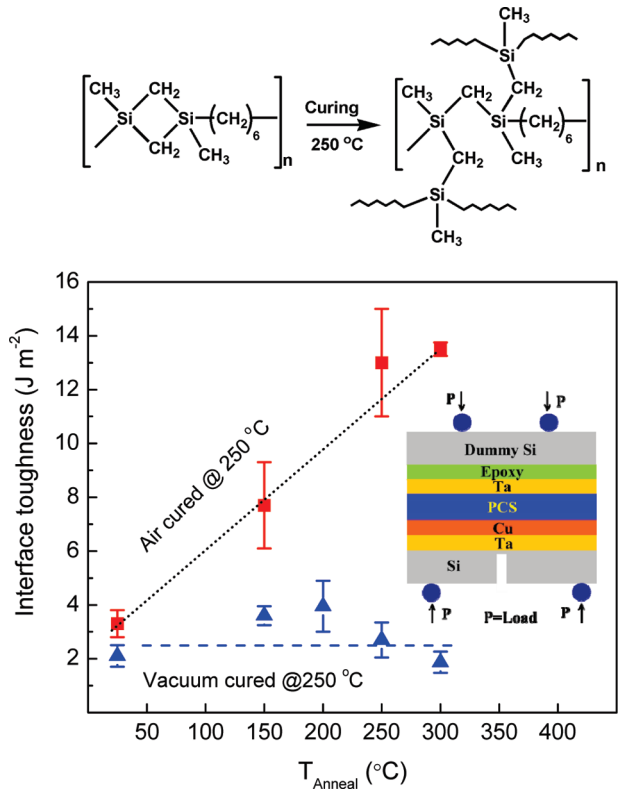

FIGURE 1. Average interface fracture toughness plotted as function of the postcure annealing temperature T_{anneal}, for Ta/PCS/Cu/Ta/Si stacks, with the PCS cured at 250 °C in either air or vacuum. The dotted lines are meant only to guide the eye.

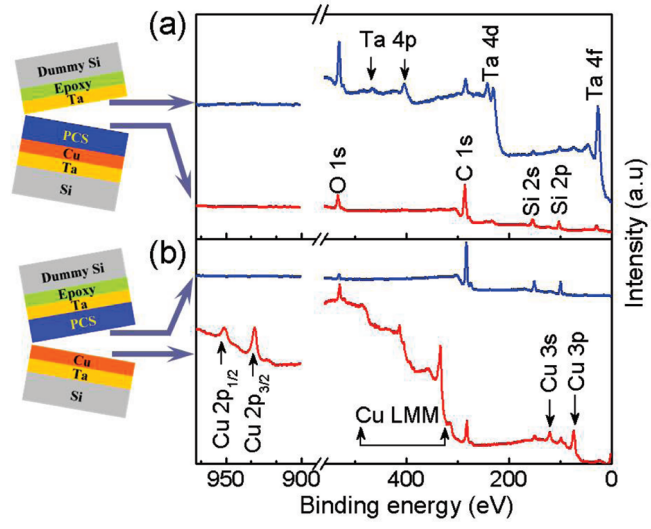

FIGURE 2. (a) XPS spectra from air-cured PCS fracture surfaces from Ta/PCS/Cu/Ta/Si stacks annealed at 250 °C. The PCS/Cu side fracture surfaces show Si, O, and C along with Ta, whereas the Ta/PCS side fracture surfaces show Si, O, and C along with Ta core-level bands. (b) XPS spectra from vacuum-cured PCS fracture surfaces from Ta/PCS/Cu/Ta/Si stacks annealed at 250 °C. The PCS/Cu side fracture surfaces show Cu, Si, O, and C along with Cu LMM Auger peaks, whereas Ta/PCS side fracture surfaces show Si, O, and C core-level bands.

3. RESULTS AND DISCUSSION

The spin-coated CLPCS polymer was cured either in air or vacuum at $T_{curing} = 250$ °C to obtain a cross-linked PCS film. Figure 1 plots the fracture toughness of Si/epoxy/Ta/

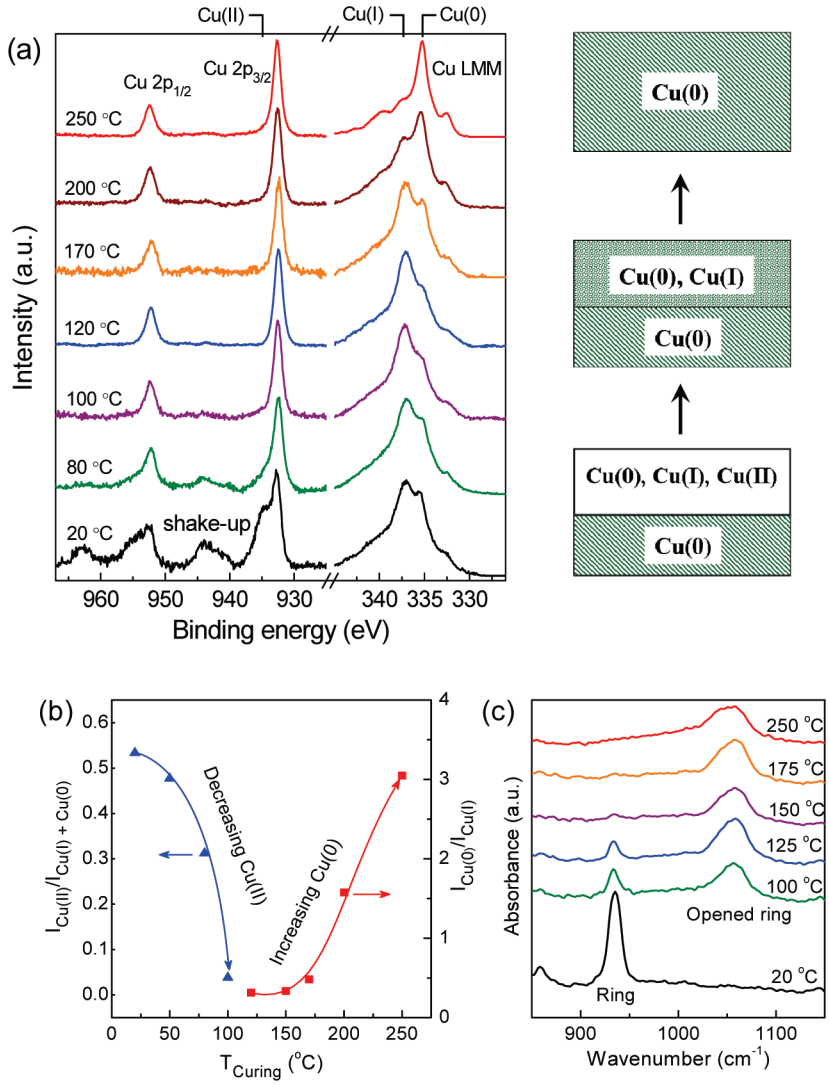

FIGURE 3. (a) Cu 2p core-level and Cu LMM Auger peak characteristics from ~3−5 nm thick PCS on copper upon curing in vacuum at different temperatures T_{curing}. (b) Relative intensities of Cu(II) and Cu(0) plotted as a function of T_{curing} determined from Gaussian peak fits. (c) FTIR spectra capturing PCS ring-opening during vacuum curing.

PCS/Cu/Ta/Si stacks (9) determined from load−displacement curves obtained from four-point bend tests as a function of postcuring anneal temperature T_{anneal} (see the Supporting Information, Figure S1). Nonannealed Ta/PCS/Cu/Ta/Si stacks with either air-cured or vacuum-cured PCS show a low interfacial toughness $G_{nonannealed}$ ~3 J/m^2 (the data points at T_{anneal} = 25 °C in Figure 1), comparable to that of Cu-silica interfaces. Stacks with air-cured PCS exhibit a monotonic toughness increase with increasing T_{anneal}. For T_{anneal} = 250 °C, we obtain $G_{250\ °C} \approx 13$ J/m^2, which is more than 4-fold higher than $G_{nonannealed}$. In contrast, the fracture toughness of vacuum cured PCS-Cu interfaces remains $\lesssim$4 J/m^2 for 150 °C $\leq T_{anneal} \leq$ 400 °C. The curing ambient also has an effect on the dielectric permittivity of the film. Vacuum-cured PCS films exhibit $k \approx 2.4$ (see the Supporting Information, Figure S2) while air-cured PCS films show ~12% higher k value of ~2.7. We note that both k values are attractive for nanodevice wiring applications.

Core-level spectra acquired by XPS from fracture surfaces of film stacks with air-cured PCS reveal cohesive PCS fracture near the Ta−PCS interface, indicating that the measured fracture energy represents a lower-bound estimate of the PCS−Cu interface toughness. This is seen from the fact that both fracture surfaces show Si 2p bands from PCS, and Ta 4f peaks (Figure 2a). Photoelectron escape depth analyses based on spectra acquired at different takeoff angles to the fracture surfaces show that fracture occurs within ~1.6 nm from the Ta−PCS interface (see supplemental Figure S3). Spectroscopic analyses further reveal that the observed annealing-induced fracture toughness increase is due to Ta−PCS interface strengthening resulting from Ta−carbon and Ta−oxygen intermixing across the Ta−PCS interface for 100 °C $\leq T_{anneal} \leq$ 300 °C (see the Supporting Information, Figure S4). For T_{anneal} > 300 °C, no interfacial delamination is observed. Instead, the crack from the notch cuts the entire sample into two pieces, confirming that the measured values at lower T_{anneal} represent a good lower bound estimate of PCS-Cu interface toughness.

In contrast, stacks with vacuum-cured PCS delaminate at the PCS−Cu interface. One fracture surface predominantly shows high Cu 2p intensity with traces of Si, while the other fracture exhibits a high intensity Si 2p band from PCS,

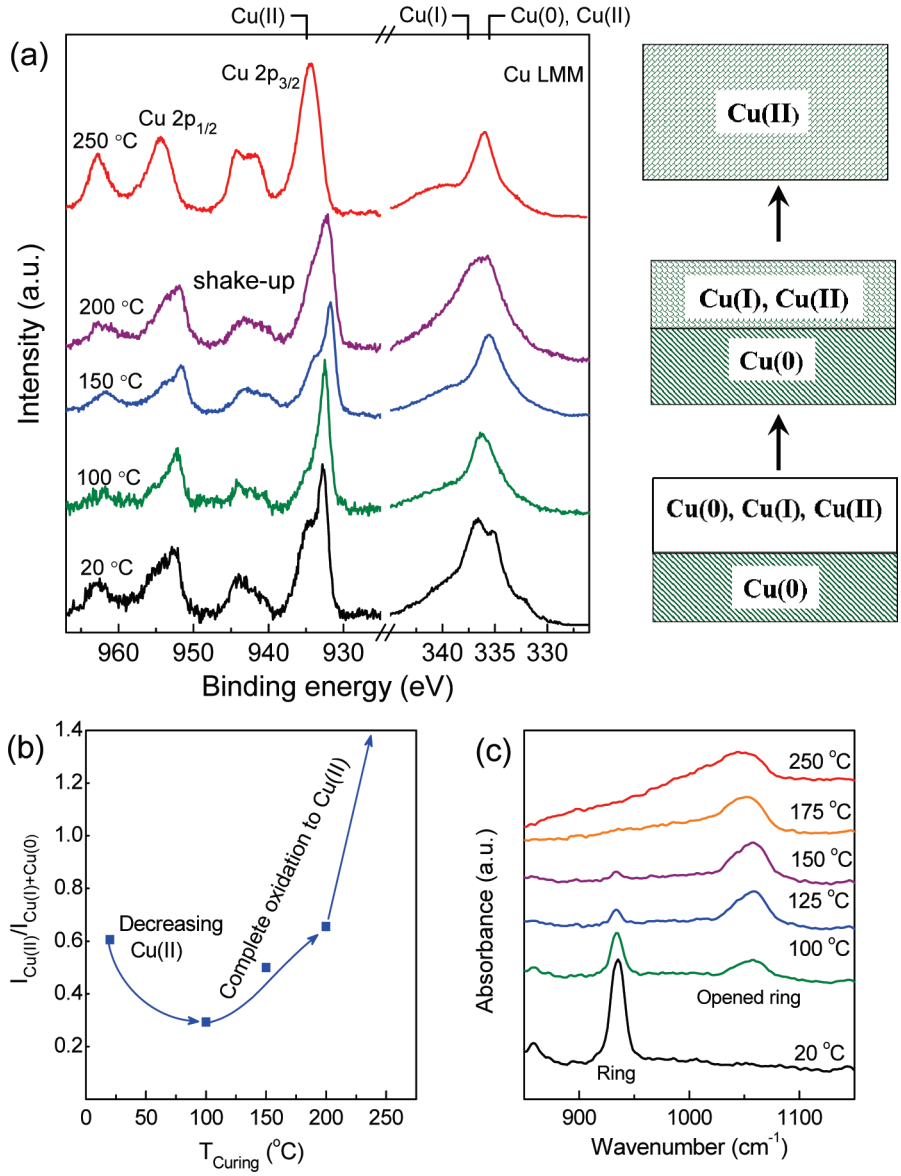

FIGURE 4. (a) Cu 2p core-level spectra from ~3−5 nm PCS on copper upon air curing at different temperatures T_{curing}. (b) Intensity ratio of Cu(II) with respect to Cu(0) and/or Cu(I) as a function of T_{curing}. (c) FTIR spectra of air-cured PCS showing ring-opening by the disappearance of the peak at 930 cm^{-1} and appearance of broad peak at 1050 cm^{-1}.

together with traces of Cu (see Figure 2b). No Ta is detectable on either fracture surface, indicating delamination near the PCS−Cu interface. Thus, for the vacuum curing case, we obtain a direct measure of the PCS−-Cu interface toughness. The insensitivity of PCS−Cu interface toughness to postcure anneals indicates that interface chemical changes during curing determine the PCS−Cu interface toughness.

In order to obtain an atomic-level understanding of the effect of the curing environment on PCS-Cu interface toughness, we studied vacuum- and air-curing of a ~3−5 nm thick CLPCS films on Cu surfaces for 25 °C < T_{curing} ≤ 250 °C using XPS and infrared spectroscopy. The low thickness of the polymer layer allows us to obtain information regarding the Cu oxidation states at the PCS−Cu interface. XPS and infrared spectra reveal surface copper oxide reduction and concomitant DSCB ring-opening in CLPCS with increasing curing temperature. The as-prepared samples exhibit all three Cu oxidation states, namely, Cu(II), Cu(I) and Cu(0). Vacuum curing at T_{curing} ~100−120 °C reduces Cu(II) to Cu(I), indicated by decreased intensities of the Cu 2p subband at ~934.5 eV and its ~943 eV shakeup along with an intensity increase in the Cu(I) LMM Auger signature at ~337.3 eV (see Figure 3a). Vacuum curing between 120 °C < T_{curing} ≤ 250 °C reduces Cu(I) to Cu(0), seen from the Cu(0) LMM Auger band intensity increase at ~335 eV (20, 21) at the expense of the Cu(I) signature. Figure 3b captures the intensity decrease and extinction of the Cu(II) state below 120 °C, and a Cu(0) increase for 120 °C < T_{curing} ≤ 250 °C. Such scavenging of surface oxide using a low k polymer could be attractive for decreasing the surface-scattering induced resistivity of copper films with feature sizes below 50 nm (22, 23).

Copper reduction, i.e., Cu(II) →Cu(I) →Cu(0), is accompanied by DSCB ring-opening, indicated by the infrared spectra (see Figure 3c) from vacuum-cured CLPCS on copper in the same temperature range. In particular, the $-CH_2-$

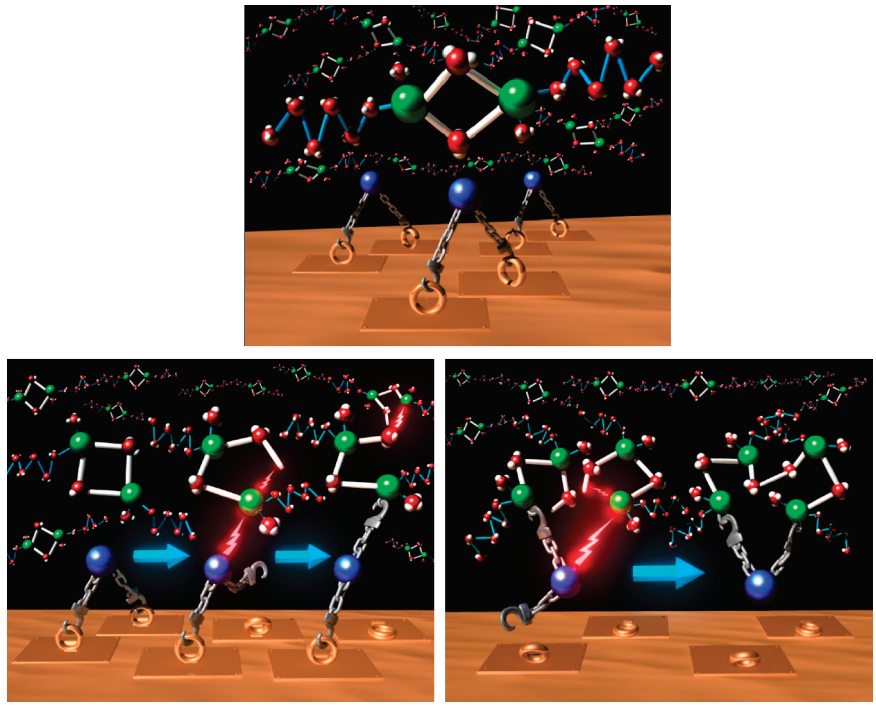

FIGURE 5. Schematic illustrations capturing salient features of the hypothesized mechanism of oxygen-mediated DSCB ring-opening and anchoring to the copper surface. Top: CLPS molecules on oxidized copper surface before curing. Bottom left: Air curing results in Cu-surface catalyzed ring-opening and Cu(II) → Cu(I) reduction. The open ring moieties cross-link with each other forming a low k dielectric, and also anchor onto the copper surface, providing strong interfacial adhesion. Bottom right: Vacuum curing reduces Cu(I) to Cu(0), precluding the bonding of opened ring moieties with the metal surface. Legend: green balls, silicon; blue balls, oxygen; red balls, carbon; white balls, hydrogen.

wagging mode at ~930 cm^{-1} characteristic (15, 24) of the DSCB ring decreases in intensity with increasing T_{curing}, and eventually disappears at ~250 °C. The ring signature is replaced by a new 1050 cm^{-1} peak corresponding to the $-CH_2-$ mode in a linear chain. The concurrency of DSCB ring-opening with surface copper oxide reduction suggests that the two processes are correlated. Weakening of Cu═O bonds by electron transfer to the surface (reduction) and the tendency of oxygen to bond with Si in the strained DSCB rings (oxidation) are complementary processes that are likely to occur simultaneously when the rings are in the vicinity of surface oxygen. The ring-opening temperature of CLPCS on copper oxide is ~90−120 °C lower than that on metals that bond either very strongly to oxygen (e.g., Al), or do not form stable oxides (e.g., Au) (15), see the Supporting Information, Figure S5. These results suggest that interfacial oxygen atoms bound to copper initiate DSCB ring-opening by attack on the DSCB Si atoms. This is believed to result in the reduction of Cu(II) to Cu(I) and the formation of $-CH_2$ radicals, which propagate a radical chain reaction and result in polymer cross-linking through successive interaction with DSCB rings in neighboring polymer chains.

The Cu oxidation states evolve differently upon air curing a ~3- to 5-nm-thick CLPCS films on Cu. The Cu(II) sub-band intensity (shoulder centered at 934.5 eV) decreases for T_{curing} < 100 °C, but monotonically increases for higher T_{curing} (see Figure 4a, b). Cu(II) and Cu(I) are the predominant states at T_{curing} = 250 °C as indicated by the 934.5 eV band and its shakeup at ~943 eV due to oxidation caused by oxygen permeation through the polymer, in contrast to the primacy of the Cu(0) state observed for vacuum curing at the same temperature. Infrared spectra (see Figure 4c) show that air curing also induces DSCB ring-opening in the same temperature range in which Cu(II) is reduced, indicating a surface-oxygen-catalyzed ring-opening similar to that observed during vacuum curing. It is difficult to tell if DSCB ring-opening during air curing is accompanied by oxidation of the polycarbosilane film because the expected position for the Si−O−Si bending vibration overlaps with the ring-opened Si−CH_2−Si signature. Although partial oxidation of the polymer near the Cu/PCS interface is likely, the retention of the C−H stretching vibrations at ca. 2900 cm^{-1} and only a 12% lower k than that obtained for vacuum curing rule out the possibility of gross oxidation of the PCS film.

We postulate that the retention of an oxidized copper surface during air curing provides the mechanism for covalent tethering of PCS chains to the copper surface via oxygen bridges between ring-opened Si- and Cu(I) or Cu(II), i.e., through Si−O−Cu linkages (25). Such covalent bond formation at the PCS−Cu interface is consistent with the high PCS−Cu interface toughness obtained during air curing. Although our infrared spectra show no discernible signatures of such linkages at the buried polymer−metal interface, our covalent anchoring hypothesis is supported by recent work (26) showing that Si−O−Cu bond formation is energetically favored when DSCB rings are in contact with Cu. A corollary of our hypothesis is that surface oxygen depletion and Cu(0) formation would preclude polymer chains anchoring to the metal via Si−O−Cu bridges and result in low interfacial fracture toughness. This is indeed what we find upon vacuum curing: Cu(0) formation and low PCS−Cu interface toughness, thus further corroborating our hypothesis. Figure

5 schematically captures the salient features of our hypothesis. Initial curing of CLPCS on copper in air or vacuum reduces interfacial Cu(II) to Cu(I). The retention of Cu-bound oxygen atoms at the PCS−Cu interface during further curing in air provides a means to anchor the DSCB ring-opened moieties in the PCS to the copper surface, leading to a strong PCS−Cu interface. In contrast, oxygen scavenging resulting from Cu(I) → Cu(0) reduction upon further vacuum curing precludes such anchoring and leads to a weak PCS interface.

4. CONCLUSIONS

In summary, we have demonstrated an entirely new approach of promoting adhesion between metals and low *k* polymers by incorporating molecular rings in the latter, and catalytically opening them to form covalent bridges with the metal. In particular, air curing polycarbosilanes on copper results in excellent interfacial toughness, while maintaining a low *k* value of the polymer dielectric. We attribute the interfacial toughening to Si−O−Cu bridges formed by the catalytic opening of disilacyclobutane rings in PCS by oxygen bound to the copper surface. Vacuum curing also promotes catalytic ring-opening and cross-linking, but Cu(0) formation by surface oxide reduction precludes covalent anchoring of the opened moieties, and thus leads to poor adhesion. Our approach could be potentially adapted for tailoring metal/low-k polymer interfaces without intermediary layers by incorporating different types of molecular rings and catalyzing mechanisms, for applications in nanodevice wiring and packaging, wireless communications, coatings and composites.

Acknowledgment. This work was supported by the New York State Foundation for Science, Technology and Innovation (NYSTAR) through the TTIP program and an NSF grant DMR 0519081.

Supporting Information Available: Additional data showing the raw data on mechanical properties, dielectric constant of the material, and fracture spectroscopy (PDF). This material is available free of charge via the Internet at http://pubs.acs.org.

REFERENCES AND NOTES

(1) Morgen, M.; Ryan, E. T.; Zhao, J. H.; Hu, C.; Cho, T. H.; Ho, P. S. *Annu. Rev. Mater. Sci.* **2000**, *30*, 645–680.
(2) Maex, K.; Baklanov, M. R.; Shamiryan, D.; Iacopi, F.; Brongersma, S. H.; Yanovitskaya, Z. S. *J. Appl. Phys.* **2003**, *93*, 8793–8841.
(3) Huo, X.; Chen, K. J.; Chan, P. C. H. *IEEE Electron Device Lett.* **2002**, *23*, 520–522.
(4) Spencer, T. J.; Osborn, T.; Kohl, P. A. *Science* **2008**, *320*, 756–757.
(5) Grujicic, M.; Sellappan, V.; Omar, M. A.; Seyr, N.; Obieglo, A.; Erdmann, M.; Holzleitner, J. *J. Mater. Process. Technol.* **2008**, *197*, 363–373.
(6) Guyer, E. P.; Dauskardt, R. H. *Nat. Mater.* **2004**, *3*, 53–57.
(7) Dubois, G.; Volksen, W.; Magbitang, T.; Miller, R. D.; Gage, D. M.; Dauskardt, R. H. *Adv. Mater.* **2007**, *19*, 3989–3994.
(8) Kim, S. H.; Oh, S. S.; Kim, K. B.; Kang, D. H.; Li, W. M.; Haukka, S.; Tuominen, M. *Appl. Phys. Lett.* **2003**, *82*, 4486–4488.
(9) Ramanath, G.; Cui, G.; Ganesan, P. G.; Guo, X.; Ellis, A. V.; Stukowski, M.; Vijayamohanan, K.; Doppelt, P.; Lane, M. *Appl. Phys. Lett.* **2003**, *83*, 383–385.
(10) Lane, M.; Dauskardt, R. H.; Krishna, N.; Hashim, I. *J. Mater. Res.* **2000**, *15*, 203–211.
(11) Rathore, J. S.; Interrante, L. V.; Dubois, G. *Adv. Funct. Mater.* **2008**, *18*, 4022–4028.
(12) Wu, Z. Z.; Papandrea, J. P.; Singh, A. P.; Ganesan, P. G.; Apple, T.; Ramanath, G.; Interrante, L. V. *Polym. Prepr. (ACS Div. Polym. Chem.)* **2004**, *45*, 118–119.
(13) Wang, P. I.; Wu, Z. Z.; Lu, T. M.; Interrante, L. V. *J. Electrochem. Soc.* **2006**, *153*, G267–G271.
(14) Murarka, S. P.; Eizenberg, M.; Sinha, A. K. *Interlayer Dielectrics for Semiconductor Technologies*; Academic Press: New York, 2003.
(15) Wu, Z. Z.; Papandrea, J. P.; Apple, T.; Interrante, L. V. *Macromolecules* **2004**, *37*, 5257–5264.
(16) Gandhi, D. D.; Lane, M.; Zhou, Y.; Singh, A. P.; Nayak, S.; Tisch, U.; Eizenberg, M.; Ramanath, G. *Nature* **2007**, *447*, 299–U2.
(17) Volinsky, A. A.; Moody, N. R.; Gerberich, W. W. *Acta Mater.* **2002**, *50*, 441–466.
(18) Dauskardt, R. H.; Lane, M.; Ma, Q.; Krishna, N. *Eng. Fract. Mech.* **1998**, *61*, 141–162.
(19) Whelan, C. M.; Kinsella, M.; Carbonell, L.; Ho, H. M.; Maex, K. *Microelectron. Eng.* **2003**, *70*, 551–557.
(20) Laibinis, P. E.; Whitesides, G. M. *J. Am. Chem. Soc.* **1992**, *114*, 9022–9028.
(21) Deroubaix, G.; Marcus, P. *Surf. Interface Anal.* **1992**, *18*, 39–46.
(22) Timoshevskii, V.; Ke, Y.; Guo, H.; Gall, D. *J. Appl. Phys.* **2008**, *103*, 113705–4.
(23) Liu, H. D.; Zhao, Y. P.; Ramanath, G.; Murarka, S. P.; Wang, G. C. *Thin Solids Films* **2001**, *384*, 151–156.
(24) Wrobel, A. M.; Stanczyk, W. *Chem. Mater.* **1994**, *6*, 1766–1770.
(25) Although C−O−Cu bridges are also possible, mechanistic considerations suggest the predominance of Si−O−-Cu surface bonding. In particular, surface-bound O attacking the Si in DSCB rings is the most likely initial step that opens the rings and forms $-CH_2$ radicals through electron transfer to surface Cu(II) to form Cu(I). The radicals then propagate polymer cross-linking through successive interchain DSCB ring-opening steps. In the absence of an external oxygen source, the surface-bound oxygen becomes attached to a Si atom in a DSCB ring, thereby reducing Cu(I) to Cu(0) and forming Si−O−Si moieties. In the presence of external O_2, the formation of Si−O and C−O species, e.g., Si−O(H or Si), and C═O, could also occur as a result of the oxidation of some of the Si−CH_2 radicals and Si−CH_2−Si bridges.
(26) Garg, S.; Singh, B.; Liu, X.; Jain, A.; Ravishankar, N.; Interrante, L.; Ramanath, G. *J. Phys. Chem. Lett.* **2010**, *1*, 336–340.

AM1001597